Transition metal impurities on the bond-centered site in germanium

S. Decoster,[1] S. Cottenier,[1,2] B. De Vries,[1] H. Emmerich,[2] U. Wahl,[3,4] J.G. Correia,[3,4] and A. Vantomme[1]

[1] *Instituut voor Kern- en Stralingsfysica and INPAC, KULeuven, BE-3001 Leuven, Belgium*
[2] *Computational Materials Engineering (CME), Institute for Minerals Engineering (GHI), Center for Computational Engineering Science (CCES) & Jülich-Aachen Research Alliance (JARA), RWTH Aachen University, DE-52064 Aachen, Germany*
[3] *Instituto Tecnológico e Nuclear, Estrada Nacional 10, PT-2686-953 Sacavém, Portugal*
[4] *Centro de Física Nuclear da Universidade de Lisboa, Avenida Prof. Gama Pinto 2, PT-1649-003 Lisboa, Portugal*

(Dated: August 18, 2008)

We report on emission channeling experiments on ion implanted Fe, Cu and Ag impurities in germanium and *ab initio* total energy calculations. Following common expectation, a fraction of these transition metals was found on the substitutional Ge position. Less expected is the observation of a second fraction on the 6-fold coordinated bond-centered site. *Ab initio* calculated heats of formation suggest that this is the result of an impurity-vacancy defect complex in the split-vacancy configuration.

PACS numbers:

During the past decade, germanium has become an increasingly important material in semiconducting applications. When compared to silicon, dopants have a higher free carrier mobility and a lower activation temperature in Ge [1], which makes it an attractive material in metal-oxide semiconductor field-effect transistors [2, 3]. Despite intensive research, several fundamental properties of this semiconductor are still poorly known. For instance, transition metals (TMs) produce deep-level states in the semiconductor band gap and are hence detrimental for the electrical properties of integrated circuits, even in small concentrations [4]. Since the lattice site of TMs has an large influence on their electrical activity, lattice location studies are important. For Si, experimental work by many techniques has led to the conclusion that Fe, Cu and Ag impurities occupy the substitutional (S) site, near-S sites and the (displaced) tetrahedral interstitial (T) site.[5–10]. For Ge, on the other hand, the electrical behavior of TM impurities has been studied quite extensively [11], but the information about their lattice location in Ge is incomplete and contradictory. Many groups working on characterization of the induced deep level states in the Ge band gap, simply presume that they are located substitutionally because they act as multiple acceptors – in accordance with the simple valence model with the impurities on the S site ([11] and references therein). However, the full picture seems to be more complicated. From Mössbauer spectroscopy experiments after recoil implantation of ^{57m}Fe and ion implantation of ^{57}Mn in Ge, the Fe-atoms were found to occupy the S site, but also the T site and a third site believed to be related to Fe$_i$-V complexes [12, 13]. From emission channeling experiments similar to the ones presented here, a large fraction of ion implanted ^{67}Cu was found on the S site, together with a smaller fraction located halfway between the S and the bond-centered (BC) site [14]. Ab initio calculations indicate that the S site is favored over the T site for 3d-transition metals in Ge as well as in Si [15, 16]. Other theoretical studies in Ge focussed on impurity-vacancy complexes with impurities from the sp-series, with conflicting geometrical results [17, 18].

To clarify the puzzling experimental data, we present a direct lattice location study of Fe, Cu and Ag in Ge with the emission channeling (EC) technique. In an EC experiment, charged particles, emitted from an implanted radioactive isotope are guided by the potential of atomic rows and planes while traveling through the crystal. The resulting anisotropic electron emission pattern around low-index crystal directions is characteristic for the lattice site occupied by the emitting atom and is measured with a 2-dimensional (2D) energy- and position-sensitive Si detector of 22×22 pixels. The advantages of this technique are the very high accuracy due to the use of 2D-patterns instead of typical spectroscopic 1D-scans and the use of very low implantation fluences which allows us to study isolated atoms. See Ref. 19 for a review.

The radioactive isotopes ^{59}Mn, ^{67}Cu and ^{111}Ag have been implanted at the ISOLDE facility in CERN to study the lattice location of Fe, Cu and Ag, respectively. ^{59}Mn (4.6 s) rapidly decays into the long-lived β^--emitter ^{59}Fe (44.6 d), which decays to ^{59}Co, receiving an average recoil of about 200 eV. This assures that the atom gets reimplanted and is not influenced by the lattice site of its precursor. ^{67}Cu (61.9 h) decays into stable ^{67}Zn by emitting β^--particles and in a similar way ^{111}Ag (7.45 d) decays into stable ^{111}Cd. The implantations have been performed at room temperature in undoped $\langle 111 \rangle$-Ge with an energy of 60 keV to fluences of 1.0×10^{13} cm^{-2} for Fe, 6.6×10^{12} cm^{-2} for Cu and 5.0×10^{12} cm^{-2} for Ag. To obtain accurate and unambiguous results, emission patterns along the four crystal directions $\langle 100 \rangle$, $\langle 111 \rangle$, $\langle 211 \rangle$ and $\langle 110 \rangle$ were measured, analyzed consistently and fitted to a set of simulated spectra. These simulations have been performed for several high-symmetry sites such as the S, T, BC,

hexagonal (H) and the so called AB, SP, Y and C sites [20], as well as for small discrete displacements between these sites along the ⟨111⟩-, ⟨100⟩- and ⟨110⟩-direction. More information about the simulations can be found in Ref. 21. To monitor the thermal stability of the lattice location of the implanted impurities, the measurements were performed on as-implanted samples, as well as on samples annealed up to 500°C in vacuum ($< 10^{-5}$ mbar) during 10 min.

Figures 1 (a)-(d) show the normalized electron emission patterns around the ⟨111⟩, ⟨100⟩, ⟨110⟩ and ⟨211⟩-axes for Ag in Ge. In all directions, an increased normalized yield along the measured axis is visible (i.e. axial channeling), indicating that at least a fraction of the implanted Ag-atoms will be located substitutionally. However, comparing the experimental patterns on panels (a) to (d) with the simulated patterns for purely substitutional Ag-atoms on respectively panels (e), (g), (i) and (k) reveals a number of discrepancies. The experimental pattern along the ⟨110⟩-direction shows a split channeling peak in the middle of panel (c) – which is not present in the simulation on panel (i) – while along the ⟨100⟩-direction the measured axial channeling effect on panel (b) is much less pronounced than the simulated one on panel (g). More discrepancies can be found by investigating the measured planar channeling effects. This visual analysis indicates that the Ag-impurities will occupy at least a second high-symmetry site. Therefore, a quantitative fitting procedure has been applied, allowing the Ag atoms to occupy up to three different sites within the Ge lattice. Adding either T, H, SP, AB, Y or C sites to the substitional fraction results only in an insignificant fit improvement (χ^2-improvement $< 2\%$), while adding a fraction on the BC site remarkably improves the fit in all directions, as has been quantified in Tab. I (columns '+BC'). Visual inspection of the simulations for the S and BC site in Fig. 1 (e)-(l), shows that overlapping these simulations will solve the discrepancies described above, leading to the acceptably accurate fits in Fig. 1 (m)-(p). Adding more high-symmetry sites results in only marginal improvements of the fits (i.e. χ^2-improvement $< 2\%$), allowing us to conclude that only very small Ag-fractions ($< 3\%$) occupy other high-symmetry sites. Allowing displaced S and/or BC sites, results in only marginally improved fits as can be seen in Tab. I (columns '+Δ'), which are too small to be physically relevant.

In the best fit to the experimental patterns, 21(3)% of the implanted Ag-atoms occupy the S site and 33(4)% the BC site. The remaining fraction, denoted as the *random* fraction, will be discussed in the next paragraph. After analyzing the patterns for Fe, Cu and Ag as implanted and after several annealing stages, the general trend is clear (Fig. 2): the three TMs are partially found on the S site and partially on the BC site.

Heavy ion implantation produces highly damaged regions, especially in materials with small lattice binding energies such as Ge, even for the low fluences used in this study. This implantation damage has a dual influence on the results shown here, and more specifically on the random fraction. Firstly, due to the deterioration of the crystal structure, β-particles from the radioactive isotopes located in damaged regions, will be emitted much more isotropically. Secondly, a fraction of the electrons emitted by the impurities on high-symmetry sites in an undamaged region will pass through damaged crystal regions, enhancing the probability for dechanneling. Both effects will result in an isotropic background to the patterns and consequently in an increased random fraction, observed in the experiments. Such a random fraction will not influence the anisotropy in the patterns nor the qualitative analysis of the high-symmetry sites in any way. This damage effect implies that the fractions presented in this work should be treated as lower limits to the real fractions. The increasing fraction of TMs on high-symmetry sites after the first annealing steps (Fig. 2) indicates that the implantation damage was at least partly recovered. The drastic decrease of this fraction in the case of Ag (Fig. 2(c)) after annealing at 500°C is related to the diffusion of Ag-atoms and will not be discussed in more detail here.

	⟨100⟩		⟨110⟩		⟨211⟩		⟨111⟩	
	+BC	+Δ	+BC	+Δ	+BC	+Δ	+BC	+Δ
as impl.	6%	1%	8%	2%	4%	2%	2%	0%
300°C	25%	3%	19%	4%	10%	3%	4%	0%
400°C	25%	2%	12%	4%	10%	3%	4%	0%

TABLE I: Relative χ^2-improvements for the best fits to the experimental patterns of the Ag-implanted sample after allowing a bond-centered Ag-fraction (+BC) in addition to the S fraction, and after further allowing displacements of the BC and S sites (+Δ).

In accordance with the studies discussed in the introduction [11–15], we found a large fraction of the TMs on the S site in Ge after ion implantation. The prevalence of the S site is consistent with theoretical work[15, 16] where the S site was found to be more favourable than the T and H sites. More intriguing, however, is the occupation of the BC site, for which we found no experimental evidence in literature. In order to understand the existence of this BC site, a complementary *ab initio* study has been performed.

We have calculated the heat of formation of 3 impurity sites in Ge: the S site, the T site and the impurity on the S site with one vacancy in the nearest neighbor shell (S+V). This latter complex was taken into account because ion implantation produces a large amount of vacancies, which are mobile at room temperature in Ge [22] and might be trapped by impurities. The heats of

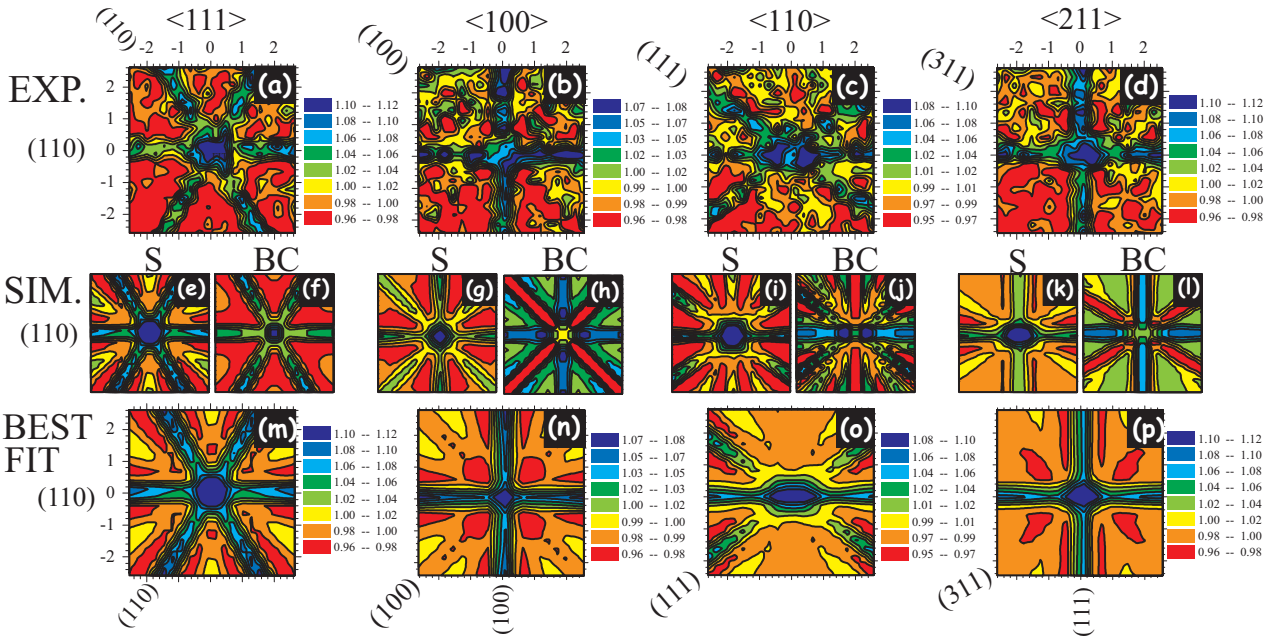

FIG. 1: (Color online) (a)-(d) Two-dimensional electron patterns emitted from ^{111}Ag in Ge around the ⟨111⟩, ⟨100⟩, ⟨110⟩ and ⟨211⟩-axes, following a 400°C annealing step in vacuum; (e)-(g) simulated patterns for Ag on the S site and (h)-(j) on the BC site around the ⟨100⟩, ⟨110⟩ and ⟨211⟩-axes; (k)-(n) the best fits to the experimental patterns. The normalized yield in the patterns is depicted with a color scale between red (low) and blue (high).

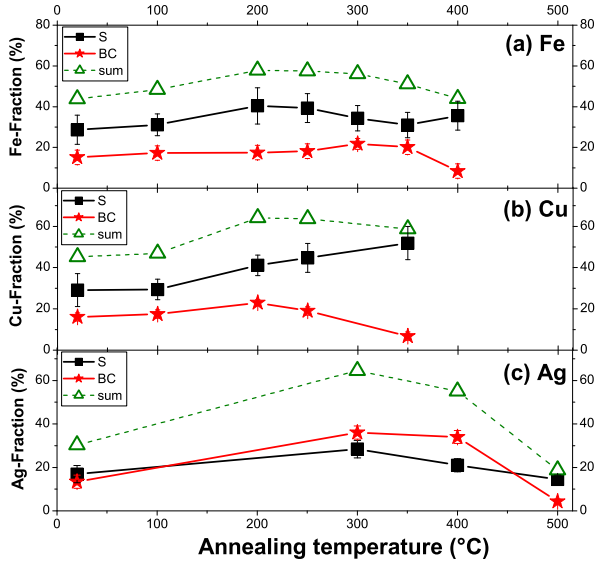

FIG. 2: (Color online) Fraction of the implanted Fe (a), Cu (b) and Ag-atoms (c) on the S site (■) and the BC site (★) in Ge, together with the total fraction (△ = ■ + ★) on high-symmetry sites, as a function of annealing temperature.

formation reported in Tab. II are calculated according to

$$\Delta H_f = E_{sup}^{imp} - \mu_{imp} - \left(32E_{sup}^{id} - n\mu_{Ge}\right) \qquad (1)$$

where E_{sup}^{imp} is the total energy of a 64-atom supercell (63 atoms if a vacancy is present) that contains the impurity, E_{sup}^{id} is the total energy of a pure Ge unit cell (diamond structure, 2 atoms), μ_{Ge} is the chemical potential of Ge (here taken equal to the total energy per atom in bulk Ge), n is the number of Ge atoms in the ideal 64-atom supercell that are replaced by either vacancies or impurities ($n = 1, 2$) and μ_{imp} is the chemical potential of the impurity with respect to the elemental solid (ferromagnetic bcc-Fe, fcc-Cu, fcc-Ag). For all elemental solids, the lattice constant was optimized and fixed for the 64-atom cells, but all atoms in those supercells were allowed to move to their equilibrium positions. The calculations were done by the APW+lo [23] method within Density Functional Theory [24, 25], as implemented in the WIEN2k code [26]. The Perdew-Burke-Ernzerhof [27] exchange-correlation functional was used, the k-space sampling was done on a 4×4×4 mesh in the 64-atom cell, and a basis set corresponding to $K_{max} = 3.5$ a.u. was taken. The influence of the size of the supercell (up to 256 atoms) on the calculations was verified and found to be negligible.

After relaxation of the configuration with the impurities on the S and the T site, no large displacements were found as can be seen from Tab. II. A slightly reduced distance to the first nearest neighbor (d) shell has been calculated in the case of the substitutional impurity, while having the impurity on the T site resulted in a small lattice expansion. This is in agreement with previous calculations for Fe in Ge [15, 16]. Adding a vacancy to the substitutional impurity (S+V), induces a large force on

	Fe		Cu		Ag	
	ΔH_f (eV)	d (%)	ΔH_f (eV)	d (%)	ΔH_f (eV)	d (%)
S	1.73	-6.7	1.33	-4.6	1.24	+0.0
T	3.02	+0.1	1.74	+1.7	1.70	+4.8
S+V	3.68	-19.8	3.08	-13.2	2.14	-11.0

TABLE II: Heat of formation for the 3 impurity environments considered in this work (ΔH_f) and the relative displacements of the first nearest neighbor shell (d) with respect to starting configuration.

the three studied TMs along the $\langle 111 \rangle$-direction, resulting in the impurity ending up on the ideal 6-fold coordinated BC site with the vacancy *split* on the nearest neighbor positions: the *split-vacancy* configuration. As can be seen from Tab. II, relaxation of this configuration results in a large contraction of the 6 neighbouring Ge atoms.

By comparing the formation energies in Tab. II, it is clear that the three studied TMs prefer the S site to the T or BC site. At first sight, this contradicts the experimental observation of the BC site. Two arguments show this is not true, however. First, putting a vacancy near the S site spontaneously leads to the BC site. Secondly, we calculated the heat of formation for a single neutral vacancy in Ge to be 2.28 eV (see also Ref. [28]). The sum of the energies needed to create an impurity on the S site and an isolated vacancy is larger than the heat of formation of the BC site for all three TMs. Therefore, S site impurities will trap the abundant and mobile vacancies created by the implantation process, which results in the BC site.

Our results strengthen the hypothesis that the Fe-atoms are found on the T site in Mössbauer experiments [13], due to the 40 eV recoil energy, received during the β-decay of the substitutional ^{57}Mn-atoms. This recoil energy is high enough to overcome the energy barrier between S and T, but not enough to get reimplanted. Reanalysis of the spectra from an earlier EC-experiment on Cu [14], indicates a similar behavior as presented here: a large fit improvement by adding a BC fraction to the S fraction and only minor improvement after allowing displacements to the BC site, in accordance to the results obtained in this study.

In conclusion, despite the general belief that transition metals are located substitutionally in Ge, we found direct experimental evidence that the ion implanted transition metals Fe, Cu and Ag occupy the bond-centered site. Corroborated by theory, this BC fraction is attributed to impurity-vacancy complexes in the split-vacancy configuration. By investigating the heat of formation of this complex, it can be concluded that the mobile vacancies will be trapped by substitutional impurities, resulting in the spontaneous occupation of the BC site. Moreover, since most of the observed TM-related deep levels in the Ge band gap are related to substitutional impurities [11], we have presented a model to possibly deactivate the TM impurities in Ge.

This work was supported by the Fund for Scientific Research, Flanders (FWO, G.0501.07), the Concerted Action of the K.U.Leuven (GOA/2004/02), the Inter-University Attraction Pole (IUAP P6/42), the Center of Excellence Programme (INPAC EF/05/2005), the Portuguese Foundation for Science and Technology (POCI-FP-81921-2007) and the ISOLDE collaboration. S. D. acknowledges financial support from FWO-Flanders.

[1] R. Hull and J. Bean, *Germanium Silicon: Physics and Materials, Semiconductors and Semimetals*, Academic, San Diego (1999).
[2] C. Yeo, B. Cho, F. Gao, S. Lee, M. Lee, C. Yu, C. Liu, L. Tang, and T. Lee, IEEE Electron Device Letters **26**, 761 (2005).
[3] Y. Yang, W. Ho, C. Huang, S. Chang, and C. Liu, Appl. Phys. Lett. **91**, 102103 (2007).
[4] E. Simoen and C. C., *Germanium-based technologies: From materials to devices*, Elsevier, Amsterdam (2007).
[5] G. Weyer, A. Burchard, M. Fanciulli, V. Fedoseyev, H. Gunnlaugsson, V. Mishin, R. Sielemann, and the ISOLDE Collaboration, Physica B **273**, 363 (1999).
[6] U. Wahl, A. Vantomme, G. Langouche, J. Correia, and the ISOLDE Collaboration, Phys. Rev. Lett. **84**, 1495 (2000).
[7] U. Wahl, J. Correia, A. Vantomme, and the ISOLDE Collaboration, Nucl. Inst. Meth. Phys. Res. B **190**, 543 (2002).
[8] U. Wahl, J. Correia, E. Rita, J. Araújo, J. Soares, and the ISOLDE Collaboration, Phys. Rev. B **72**, 014115 (2005).
[9] N. Hai, T. Gregorkiewicz, C. Ammerlaan, and D. Don, Phys. Rev. B **56**, 4614 (1997).
[10] B. Bunker, J. Vac. Sci. Technol. A **5**, 3003 (1987).
[11] P. Clauws and E. Simoen, Mat. Sci. Semicond. Proc. **9**, 546 (2006).
[12] P. Schwalbach, M. Hartick, M. Ciani, E. Kankeleit, B. Keck, R. Sieleman, B. Stahl, and L. Wende, Hyperfine Interactions **70**, 1121 (1992).
[13] H. Gunnlaugsson, G. Weyer, M. Dietrich, M. Fanciulli, K. Bharuth-Ram, R. Sielemann, and the ISOLDE Collaboration, Physica B **340**, 537 (2003).
[14] U. Wahl, J. Correia, J. Soares, and the ISOLDE Collaboration, Physica B **340**, 799 (2003).
[15] A. Continenza, G. Profeta, and S. Picozzi, Phys. Rev. B **73**, 035212 (2006).
[16] Z. Zhang, B. Partoens, K. Chang, and F. Peeters, Phys. Rev. B **77**, 155201 (2008).
[17] H. Höhler, N. Atodiresei, K. Schroeder, R. Zeller, and P. Dederichs, Phys. Rev. B **71**, 035212 (2005).
[18] J. Coutinho, S. Öberg, V. Torres, M. Barroso, R. Jones, and P. Briddon, Phys. Rev. B **73**, 235213 (2006).
[19] U. Wahl, J. Correia, A. Czermak, S. Jahn, P. Jalocha, J. Marques, A. Rudge, F. Schopper, J. Soares, A. Vantomme, et al., Nucl. Inst. Meth. Phys. Res. A **524**, 245 (2004).
[20] U. Wahl, Phys. Rep. **280**, 145 (1997).

[21] H. Hofsäss and G. Lindner, Phys. Rep. **201**, 121 (1991).
[22] H. Hässlein, R. Sielemann, and C. Zistl, Phys. Rev. Lett. **80**, 2626 (1998).
[23] E. Sjöstedt, L. Nordström, and D. J. Singh, Solid State Commun. **114**, 15 (2000).
[24] P. Hohenberg and W. Kohn, Phys. Rev. **136**, 864 (1964).
[25] S. Cottenier, (Instituut voor Kern- en Stralingsfysica, KULeuven, Belgium) (2002), ISBN 90-807215-1-4 (freely available from http://www.wien2k.at/reg_user/textbooks).
[26] P. Blaha, K. Schwarz, G. Madsen, D. Kvasnicka, and J. Luitz, (Karlheinz Schwarz, Techn. Universität Wien, Austria) (1999), ISBN 3-9501031-1-2.
[27] J. P. Perdew, S. Burke, and M. Ernzerhof, Phys. Rev. Lett. **77**, 3865 (1996).
[28] A. Fazzio, A. Janotti, J. d. S. Antonio, and R. Mota, Phys. Rev. B **61**, R2401 (2000).